

1 Inclusion of Oxford Nanopore long reads improves all microbial and phage  
2 metagenome-assembled genomes from a complex aquifer system  
3 Will A. Overholt<sup>1</sup>, Martin Hölzer<sup>2,3</sup>, Patricia Geesink<sup>1</sup>, Celia Diezel<sup>2</sup>, Manja Marz<sup>2,3,4</sup>, Kirsten  
4 Küsel<sup>1,5</sup>

5 <sup>1</sup>Institute of Biodiversity, Aquatic Geomicrobiology, Friedrich Schiller University, Jena, Germany

6 <sup>2</sup>RNA Bioinformatics and High-Throughput Analysis, Friedrich Schiller University, Jena,  
7 Germany

8 <sup>3</sup>European Virus Bioinformatics Center, Friedrich Schiller University, Jena, Germany

9 <sup>4</sup>FLI Leibniz Institute for Age Research, Jena, Germany

10 <sup>5</sup>German Center for Integrative Biodiversity Research Halle-Jena-Leipzig, Leipzig, Germany

11 **Abstract:**

12 Assembling microbial and phage genomes from metagenomes is a powerful and appealing  
13 method to understand structure-function relationships in complex environments. In order to  
14 compare the recovery of genomes from microorganisms and their phages from groundwater, we  
15 generated shotgun metagenomes with Illumina sequencing accompanied by long reads derived  
16 from the Oxford Nanopore sequencing platform. Assembly and metagenome-assembled  
17 genome (MAG) metrics for both microbes and viruses were determined from Illumina-only  
18 assemblies and a hybrid assembly approach. Strikingly, the hybrid approach more than doubled  
19 the number of mid to high-quality MAGs (> 50% completion, < 10% redundancy), generated  
20 nearly four-fold more phage genomes, and improved all associated genome metrics relative to  
21 the Illumina only method. The hybrid assemblies yielded MAGs that were on average 7.8%  
22 more complete, with 133 fewer contigs and a 14 kbp greater N50. Furthermore, the longer  
23 contigs from the hybrid approach generated microbial MAGs that had a higher proportion of  
24 rRNA genes. We demonstrate this usefulness by linking microbial MAGs containing 16S rRNA  
25 genes with extensive amplicon dataset. This work provides quantitative data to inform a  
26 cost-benefit analysis on the decision to supplement shotgun metagenomic projects with long  
27 reads towards the goal of recovering genomes from environmentally abundant groups.

28

## Introduction

29           Shotgun metagenomics is a powerful method that conceptually allows all the genomes  
30 from all the organisms and their associated viruses within a sample to be determined with  
31 sufficient sequencing depth (Venter *et al.*, 2004; Handelsman *et al.*, 2007). In practice,  
32 metagenomic data typically represents hundreds to thousands of microorganisms and viruses at  
33 different coverage levels depending on the community structure within the sample (richness,  
34 evenness, and genome size variation). These data enable the determination of the community  
35 composition (who is there) and total community function (what are they capable of doing). In  
36 addition to this wealth of information, one of the most beneficial outcomes of shotgun  
37 metagenomic projects is the ability to assemble high quality, complete or nearly-complete,  
38 genomes from organisms not yet amenable to cultivation practices (Tyson *et al.*, 2004; Luo *et al.*  
39 *et al.*, 2012). And indeed, such metagenome-assembled-genomes (MAGs) have provided  
40 information leading to the cultivation of organisms of interest (Gutleben *et al.*, 2018; Cross *et al.*,  
41 2019; Imachi *et al.*, 2019), along with the discoveries of new metabolic processes (Daims *et al.*,  
42 2015), novel insights into the ecology and evolution of globally abundant groups (Delmont *et al.*,  
43 2018), and uncovering a wide diversity of novel Phylum-level lineages that have restructured the  
44 current understanding of the tree of life (Brown *et al.*, 2015; Hug *et al.*, 2016).

45           MAGs not only represent bacteria and archaea, but also include viruses, which are an  
46 integral part of most metagenomes (Dutilh *et al.*, 2014). Viruses are the most abundant  
47 biological entities in many ecosystems and can exert proportionately large effects on ecosystem  
48 functions (Fuhrman, 1999; Breitbart *et al.*, 2002). Viral MAGs have lead to the discovery of  
49 megaphages (with genomes >540 kb) from human and animal gut microbiomes (Devoto *et al.*,

50 2019), provided the first insights into the global distribution of such megaphages (Al-Shayeb *et*  
51 *al.*, 2019), and confirmed that environmental cyanophages contribute to global marine  
52 photosynthesis rates (Fridman *et al.*, 2017). However, the identification of viruses from  
53 metagenomes and their distinction from prophages continues to be challenging because there is  
54 not an established computational gold standard (Nooij *et al.*, 2018).

55 One exciting avenue in reconstructing *de novo* MAGs has been the inclusion of  
56 long-read sequences that can act as scaffolds to short-read sequences to help improve  
57 contiguity and bridge repeat regions within a genome (Chen *et al.*, 2019). This concept has  
58 been present since the advent of second-generation sequencing technologies (Roche 454,  
59 Illumina, SOLiD) (Goldberg *et al.*, 2006), but the breakthroughs in third-generation sequencing  
60 technologies, particularly PacBio and Oxford Nanopore Technologies (ONT), have improved the  
61 practicality of such approaches by providing access to much longer reads (Scholz *et al.*, 2014;  
62 Frank *et al.*, 2016; Bertrand *et al.*, 2019).

63 The goal of this study was to compare a hybrid assembly approach, incorporating ONT  
64 long reads, to an Illumina-only short-read approach with respect to the recovery of high-quality  
65 MAGs from a groundwater ecosystem. We leveraged the well-characterized monitoring transect  
66 of the Hanich Critical Zone Exploratory (CZE) that encompasses 15 monitoring wells spread  
67 across a hillslope covered by mixed beech forest, pasture land, and cropland (Küsel *et al.*,  
68 2016). Groundwater from this site contains a wide diversity of microbial life. The microorganism  
69 component is dominated by Patescibacteria, uncultured organisms that are often missed by  
70 routine amplicon datasets (Herrmann *et al.*, 2019; Wegner *et al.*, 2019), and the viral component  
71 has only recently started to be explored (Kallies *et al.*, 2019). A previous, gene-centric based  
72 metagenomics project has identified dominant metabolic pathways within the aquifer (Wegner *et*  
73 *al.*, 2019). However, it has been challenging to directly link these key metabolic pathways to the

74 specific microorganisms mediating them, which is critical for our understanding of the ecology of  
75 the site.

76 In order to address these knowledge gaps, we first quantified the improvements in the  
77 recovery of MAGs by including Oxford Nanopore Technology (ONT) long reads. This approach  
78 doubled the number of recovered MAGs that met our quality thresholds and covered a wider  
79 range of phylogenetic diversity present. The hybrid approach also improved all MAG metrics  
80 assessed and had a higher proportion of recovered MAGs with rRNA genes. From a viromics  
81 perspective, there were nearly four times more phages identified from the hybrid assembly, and  
82 of these, there were 10x more prophages identified. The results from this study are likely  
83 conservative and we expect there to be further improvements as ONT sequence quality  
84 increases with more accurate base calling algorithms and as more assembly and binning  
85 algorithms are developed to take advantage of all the information provided by long reads.

86

## Materials and Methods

87

### Sample Collection, DNA Extraction

88 Groundwater was collected in the Hainich Critical Zone Exploratory (NW Thuringia,  
89 Germany), from shallow groundwater resources in Upper Muschelkalk bedrock that has been  
90 extensively described (Küsel *et al.*, 2016; Lehmann and Totsche, 2020). In brief, the Hainich  
91 CZE contains a multistorey, fractured aquifer system within the hillslope, composed of alternating  
92 layers of limestone and mudstone (Kohlhepp *et al.*, 2017). The Upper-Muschelkalk aquifer  
93 system is characterized by the limestone-dominated main aquifer (Trochitenkalk formation,  
94 moTK; formerly referred to as the HTL) that is predominantly oxic and the mudstone-dominated

95 hanging strata (including Meissner formation, moM; formerly the HTU) that is anoxic (Kohlhepp  
96 *et al.*, 2017). Groundwater (115 L) was collected from well H52 (moM) on December 11th, 2018  
97 and was sequentially filtered through 0.2  $\mu$ M, and 0.1  $\mu$ M PTFE filters (142 mm, Omnipore  
98 Membrane, Merck Millipore, Germany). Filters were immediately frozen on dry ice and  
99 transported to a -80° C freezer.

100 The DNA extraction was performed as previously described, using a phenol-chloroform  
101 based method without mechanical lysis to minimize fragmentation (Taubert *et al.*, 2018).  
102 Following extraction, the Zymo DNA Clean & Concentrator kit was used to purify and  
103 concentrate the DNA for both Illumina and Oxford Nanopore Technology (ONT) sequencing.  
104 DNA concentrations of 8.89 ng/ $\mu$ L (0.1 $\mu$ M filter fraction) and 37.7 ng/ $\mu$ L (0.2 $\mu$ M filter fraction)  
105 were measured using a Qubit 4 Fluorometer (Invitrogen).

106

## Illumina Metagenome Preparation and Initial Processing

107 Illumina libraries from both filter fractions were generated using the NEBNext Ultra II FS  
108 DNA library preparation kit following the recommended protocol. Size selection was performed  
109 using the AMPure XP beads (Beckman Coulter). The average insert sizes were 509 bp (0.2 $\mu$ M  
110 fraction) and 392 bp (0.1  $\mu$ M fraction) as determined with an Agilent Bioanalyzer using a  
111 DNA7500 chip. The sequencing was performed in-house on an Illumina Miseq with 2x300 bp v3  
112 chemistry. The 0.2  $\mu$ M filter fraction DNA sample generated 17,660,385 paired-end sequences  
113 (10.6 Gbp), while the smaller 0.1  $\mu$ M fraction sample generated 15,546,350 (9.33 Gbp) raw  
114 sequences.

115 Adapter sequences from the Illumina reads were removed using bbdduk using kmer  
116 searching (k=23, hdist=1) and reads were trimmed with a phred score of 20, allowing to trim  
117 both sides of the read. Reads shorter than 50 bp were discarded (Bushnell, 2014). The average

118 estimated insert sizes of the sequences were 234 bp and 214 for the 0.2  $\mu$ M fraction and the 0.1  
119  $\mu$ M fraction samples, respectively. Raw reads were deposited at the ENA under accession  
120 PRJEB35315.

121

## Oxford Nanopore Metagenome Preparation

122 We performed Nanopore sequencing of the 0.2  $\mu$ M fraction on a single MinION flow cell  
123 (FLO-MIN106 with an R9.4.1 pore) using the 1D genomic DNA by ligation kit (SQK-LSK109,  
124 ONT) following manufacturers' instructions with minor adaptations. In short, the initial g-TUBE  
125 shearing step was omitted and potential nicks in DNA and DNA ends were repaired in a  
126 combined step using NEBNext FFPE DNA Repair Mix and NEBNext Ultra II End  
127 repair/dA-tailing Module (New England Biolabs, USA) and doubling the incubation time. A  
128 subsequent AMPure bead (Agencourt AMPure XP, Beckman Coulter) purification was followed  
129 by the ligation of sequencing adapters onto prepared ends. A second clean-up step with  
130 AMPure beads was performed and sequencing buffer and loading beads were added to the  
131 library. An initial quality check of the flow cell (ID: FAK43462) showed 1761 active pores at the  
132 start of sequencing. We loaded the DNA with a concentration of 98 ng/ $\mu$ l (measured by Qubit 3  
133 Fluorometer; Thermo Fisher Scientific) and a total amount of  $\sim$ 1.4  $\mu$ g. The sequencing run  
134 stalled after 18 h and was restarted for another 24 h using the MinKNOW software.

135 Basecalling was performed using the Guppy software (v2.3.1) with the high-accuracy  
136 model r9.4.1\_450bps\_large\_flipflop. Called reads were classified as either pass or fail  
137 depending on their mean quality score. A total of 2,380,279 reads were basecalled and of these  
138 2,081,879 (87.5%) were passed as satisfying the quality metric. The passed reads contain a  
139 total of 11.58 Gb of DNA sequence with a mean read length of 5,560 nt. This passed-fraction  
140 amounts to 91.8% of the total DNA nucleotide bases sequenced.

141 We deposited the raw signal files (FAST5) and basecalled reads (FASTQ) at the ENA  
142 under accession PRJEB35315.

143

## Metagenome Assembly and Binning

144 We used metaSPAdes v3.13.0 (Nurk *et al.*, 2017) to assemble the hybrid and  
145 Illumina-only data in order to be able to directly compare both approaches. The sequences from  
146 the 0.2  $\mu$ m sample were individually assembled with the default parameters specified by the  
147 “-meta” flag with only the inclusion of the long reads with the “-nanopore” flag being different.  
148 The assembly statistics for the two methods were calculated using MetaQUAST with the default  
149 settings (Mikheenko *et al.*, 2016). We binned the scaffolds from each assembly that were longer  
150 than 1000 nucleotides (nt) using MaxBin2 (Wu *et al.*, 2016) and MetaBAT2 (Kang *et al.*, 2015,  
151 2019) included in the MetaWRAP (Uritskiy *et al.*, 2018) binning module with the “--universal”  
152 flag. Differential coverage information was included using Illumina QA/QC reads from both filter  
153 fractions. Additionally, scaffolds > 3000 nt from each assembly were binned with BinSanity using  
154 the “wf” workflow and the log normalized coverage file produced with the “BinSanity-profile”  
155 command (Graham *et al.*, 2017). The MetaWRAP “Bin\_refinement” module was used to  
156 dereplicate bins produced from the 3 different binning methods, using the MetaWRAP scoring  
157 algorithm which favors low redundancy values while also selecting for higher percent  
158 completion. We found that the MetaWRAP “Ressamble\_bins” module reduced the quality of our  
159 bins and thus proceeded with the two sets of refined bins that were at least 50% complete with  
160 less than 10% redundancy.

161 Each collection was imported into Anvi'o and MAG statistics were exported using the  
162 anvi-summarize command (Murat Eren *et al.*, 2015). Our completeness and  
163 redundancy/contamination criteria were initially assessed using estimations from checkM (Parks

164 *et al.*, 2015), while the estimations exported from anvio were used to calculate the values  
165 represented in Figure 1 (visualized using the R package ggplot2 v3.1.0 (Wickham, 2009;  
166 Wickham *et al.*, 2019)). The anvio completeness estimations were lower than the checkM  
167 values while the redundancy/contamination estimations were higher, and therefore 74 hybrid  
168 and 39 Illumina-only MAGs were included, out of the original 82 and 44. Each MAG was  
169 screened for rRNA genes using barrnap, with each hit required to be at least 20% of the full  
170 gene length (Seemann, 2015). These statistics were compiled from the automatically refined  
171 MAGs and not from manually curated MAGs as we considered this the most direct comparison.  
172 While we consider it essential that MAGs be manually curated before publishing (Bowers *et al.*,  
173 2017; Shaiber and Eren, 2019), using the automated results for this specific comparison  
174 minimizes added bias, and likely underestimates the actual improvements due to the more  
175 fragmentary nature of the Illumina-only MAGs.

176 To identify MAGs that were recovered from both assembly methods, FastANI was run on  
177 all pairwise comparisons of MAGs that were initially assessed using checkM (82 hybrid, 44  
178 Illumina-only) (Jain *et al.*, 2018). All MAGs that were recovered from both assemblies had an  
179 average nucleotide identity (ANI) of at least 98.8%, and in all cases, secondary hits were < 82%  
180 ANI. These shared MAGs were investigated in more detail as they enabled a direct comparison  
181 between the Illumina and the hybrid assemblies. Paired Welch's t-tests with  
182 Benjamini-Hochberg correction were used to specifically test the differences in completeness,  
183 redundancy/contamination, genome length, number of scaffolds, and N50. The proportion of  
184 MAGs containing each of the rRNA genes was tested using a two-sample z-test in R (R Core  
185 Team, 2014).

186 The scaffolds from each pair of MAGs that were recovered were aligned using mummer  
187 wrapped within the mummer2circos.py (<https://github.com/metagenlab/mummer2circos>) script



188 (Kurtz *et al.*, 2004). All nanopore reads > 1 kbp were aligned to a concatenated fasta file of all  
189 scaffolds from all the hybrid-generated bins using minimap2 with the “-ax map-ont” flag (Li,  
190 2018). Log2 scaled coverage profiles were generated from QAQC Illumina reads for each filter  
191 fraction using pileup.sh across 1 kb sized sections from the BBTools suite (Bushnell, 2014),  
192 after aligning the reads to the hybrid-bin scaffolds using bbmap.sh and sorting the alignments  
193 with samtools (Li *et al.*, 2009). MAGs were taxonomically classified using GTDB-TK v0.3.2,  
194 following the classify workflow (Hyatt *et al.*, 2010; Matsen *et al.*, 2010; Price *et al.*, 2010; Eddy,  
195 2017; Jain *et al.*, 2018; Parks *et al.*, 2018).

196 The 16S rRNA genes recovered from MAGs were compared using blastn to 97%  
197 representative operational taxonomic units (OTUs) from primer pair 341F/785R (Altschul *et al.*,  
198 1990; Yan *et al.*, 2019). All hits were required to be >98.5 % sequence identity across at least  
199 350 bp. In the case of multiple OTUs matching a MAG 16S gene, the highest bit score was  
200 used, followed by the most abundant representative OTU. The representative OTUs originated  
201 from 101 samples collected between July 2014 and April 2017 from 10 monitoring wells of the  
202 hillslope transect (Yan *et al.*, 2019). The figure was created using ggplot2 and the tidyverse  
203 package within R (R Core Team, 2014; Wickham *et al.*, 2019).

204 In order to disentangle the improvements in MAG recovery due to longer ONT scaffolds  
205 instead of simply having higher sequencing depth, we subsampled the ONT reads into four  
206 different sets, then re-ran the SPAdes assemblies and binning steps. As described above, the  
207 full hybrid assembly approach was based on 17,660,385 Illumina paired-end sequences (10.6  
208 Gbp), and 2,081,879 ONT sequences (11.58 Gbp). The four additional ONT sets were, (1) all  
209 nanopore reads >10,000 nt which lead to 349,321 sequences (6.8 Gbp), (2) ONT reads >  
210 20,000 nt (114,853 sequences; 3.6 Gbp), (3) ONT reads > 50,000 nt (7,848 sequences; 0.48  
211 Gbp), and (4) randomly subsampled to 25% of the initial number of sequences (595,070

212 sequences, 3.15 Gbp). Each of the resulting assemblies were binned and analyzed following  
213 the same procedures as above.

214

## Viral Comparison

215 We used VirSorter v1.0.5 to search for putative phage and prophage sequences in the  
216 assemblies (Roux *et al.*, 2015). To identify the phages that were recovered from both  
217 assemblies, we used Blastn v2.9.0+ and filtered the hits by an e-value of 1e-10, a sequence  
218 identity >90%, and an alignment length >50% (Altschul *et al.*, 1990).

219

## Results and Discussion

220 One of the most striking findings is that the inclusion of long reads more than doubled  
221 (74 vs 39) the number of bacterial and archaeal MAGs that were at least 50% complete and  
222 less than 10% redundant, as compared to using assemblies generated from only Illumina  
223 short-read sequences (Figure 1 A). The 74 MAGs recovered from the hybrid approach were  
224 less fragmented with more than 50% having less than 100 scaffolds as compared to ~5% of the  
225 Illumina-only MAGs (Figure 1 B). The hybrid MAGs correspondingly exhibited much higher N50  
226 values with > 75% of the MAGs having an N50 > 10 kbp as compared to 20% of the  
227 Illumina-only MAGs (Figure 1 C). The additional MAGs recovered from the hybrid approach  
228 were due to recovering MAGs with lower coverages (minimum 1.9x vs 4.2x) and improved  
229 recovery of populations that were close to our quality cutoff values (Figure 1 E).

230

231 In addition to the bacterial and archaeal MAGs, we identified 278 putative phage  
232 sequences (258 phages, 20 prophages) in the hybrid assembly and only 73 (71 phages, 2  
prophages) in the Illumina-only assembly (Figure 1 F). Remarkably, the number of complete

233 phage contigs of the VirSorter category 1 (confident phage assignment) increased from 7 to 22  
234 sequences in the hybrid assembly. Thus, the integration of long-read data into the assembly  
235 process helped to recover more potential phage sequences from the sample, as well as an  
236 increase in phage sequences that were confidently identified. In one noteworthy case, a  
237 category 2 phage sequence (enriched in viral domains) from the Illumina-only assembly (length  
238 17,648 nt) was integrated into a much larger prophage contig (category 4; high confidence  
239 prophage) within the hybrid assembly (75,806 nt). Of the 73 identified putative phage  
240 sequences from the Illumina-only assembly, 52 were also recovered with the hybrid approach.  
241 The remaining 21 phage sequences are composed of three category-1, 17 category-2, and a  
242 single category-4 prophage. Of those, 19 sequences could be confirmed by an additional blast  
243 step to be included in larger contigs of the full hybrid assembly, however, they were not  
244 identified by VirSorter within the hybrid assembly.

245 For the bacteria and archaea, every MAG reconstructed from the Illumina-only assembly  
246 was also recovered from the hybrid assembly. We performed an in-depth comparison of the 44  
247 bacteria and archaea MAGs that were initially recovered with both assemblies (Table S1). On  
248 average, the hybrid-assembled MAGs were  $7.8\% \pm 3.1\%$  (mean  $\pm$  95% confidence intervals)  
249 more complete (adj.p <  $1e-5$ ) and exhibited the same degree of redundancy ( $0.4\% \pm 0.7\%$ ; adj.p  
250 = 0.22). In addition, the hybrid MAGs were  $358 \pm 123$  kbp longer (adj.p <  $1e-5$ ), with  $133 \pm 34$   
251 fewer scaffolds (adj.p <  $1e-8$ ), that had  $14.1 \pm 5.4$  kbp greater N50 values (adj.p <  $1e-5$ ). There  
252 was no significant difference found in the proportion of the rRNA genes between the recovered  
253 MAGs (two proportion two-tailed z-test), although the hybrid MAGs had 1 more 5S gene (16 vs.  
254 15), 6 more 16S genes (16 vs. 10), and 4 more 23S genes (13 vs. 9). A non-significant result is  
255 not discouraging here as even a single extra 16S rRNA gene might allow a dominant population  
256 to be connected to an extensive amplicon dataset. In addition, a manual examination of the few

257 Illumina-only MAGs that were more complete than the corresponding hybrid MAG found that the  
258 Illumina-only MAGs were likely mixed populations with different coverage profiles across their  
259 scaffolds.

260 To see if the improvements in MAG-retrieval were mainly due to the increase in  
261 sequencing depth provided by the ONT reads, we subsampled using four different strategies.  
262 These ranged from only using ONT reads > 50,000 nt (7,848 sequences; 0.48 Gbp) to all reads  
263 > 10,000 nt (349,321; 6.8 Gbp), along with a random subsampling to simulate a less successful  
264 sequencing run (595,070 sequences; 3.15 Gbp) (Table S2). The randomly subsampled ONT set  
265 yielded 62 MAGs that were > 50% complete and < 10% redundancy (as assessed by checkM),  
266 32 more MAGs than the MiSeq assembly alone. Including only the ~8,000 reads that were  
267 greater than 50,000 nt resulted in 58 MAGs passing our standards. We interpret these results to  
268 show that the longer nanopore reads do help recover MAGs, and a large improvement can be  
269 expected even if the ONT run was not so successful, while also acknowledging that the greater  
270 sequencing depth alone supplied by the ONT reads partially contributes to these results.

271 The full hybrid assembly recovered MAGs representing 17 phyla, while 14 phyla were  
272 represented from the Illumina-only assembly. The missing phyla were Bacteroidota (2 MAGs),  
273 Microarchaeota (1), and Verrucomicrobiota (1). The (super)phylum with the greatest  
274 improvement in the number of assembled MAGs was the Patescibacteria (formerly the  
275 Candidate Phyla Radiation group), with over double (35 vs. 17) the number of MAGs recovered  
276 from the hybrid approach that met our criteria (Figure 2). The ONT long-read sequences bridge  
277 missing gaps in the Illumina-only MAGs, thereby improving the contiguity and increasing the  
278 genome length across fewer scaffolds (Figure 2). It is noteworthy that these benefits are not  
279 restricted to only the most abundant organisms and even relatively few long-reads mapping to  
280 populations can improve chances to recover them (Figure 2 B). Here we focused on the

281 Patescibacteria, since this group contains almost no cultivated representatives and they are  
282 often highly abundant in groundwater systems (Brown *et al.*, 2015; Pedron *et al.*, 2019). In  
283 addition, previous research from the Hainch CZE has demonstrated that Patescibacteria can  
284 represent up to 79% of the groundwater community (Herrmann *et al.*, 2019).

285 A similar visualization was performed for three other dominant bacterial phyla  
286 (Nitrospirota, Actinobacteriota, Proteobacteria) that had previously been shown to be important  
287 in the functioning of the groundwater (Wegner *et al.*, 2019; Yan *et al.*, 2019) (Figure S1). There  
288 were almost double the number of Nitrospirota associated MAGs (7 vs. 4) recovered with the  
289 hybrid approach, and these were amongst the largest of the MAGs recovered. Within the  
290 Actinobacteriota and Proteobacteria, we recovered the same MAGs with each approach. The  
291 MAG metrics within each phyla fell within the confidence intervals of the full sample set with the  
292 exception of the Actinobacteriota that showed greater than expected improvements with the  
293 hybrid approach (Figure S1). The results presented herein also likely further underestimate the  
294 improvements ONT long reads contribute since the 2x300 bp paired-end sequences used are  
295 longer than those typically generated in metagenome projects (either 2x150 reads from an  
296 Illumina HiSeq or 2x250 from an Illumina Nextseq).

297 Our results from these diverse and understudied groundwater ecosystems extend  
298 findings recently published that utilized mock communities and spiked-in complex human gut  
299 microbiome communities (Bertrand *et al.*, 2019). We demonstrate the recovery of a wider  
300 diversity of microorganisms and phages using a hybrid approach, in our case, the recovery of  
301 three additional phyla and 6 classes. Additionally, the improvements towards contiguity and  
302 completeness of recovered MAGs are likely generalizable as they are reflected within the  
303 results presented by Bertrand and colleagues (2019). While not explicitly tested in our study, the

304 hybrid approach has been previously shown to result in fewer misassemblies using a mock  
305 community where the genome contents are known *a priori* (Bertrand *et al.*, 2019).

306 High-quality MAGs that are (nearly) complete with lower frequencies of misassemblies  
307 allow relevant metabolic processes to be constrained to individual organisms, directly  
308 connecting phylogeny to function (Woyke *et al.*, 2019). To help with this task, one of the benefits  
309 we document here is that the less fragmented hybrid MAGs contained more ribosomal RNA  
310 genes (Figure 1 D). 16S rRNA gene amplicon datasets are a common method to survey  
311 microbial communities, often with a large number of samples that are well replicated  
312 spatiotemporally due to decreases in sequencing costs and ease of multiplexing. Here, MAGs  
313 were linked to a 16S dataset containing 101 samples from the Hainich CZE that were collected  
314 across 3 years (July 2014 to April 2017) and 10 wells (Yan *et al.*, 2019).

315 Of the 16S hybrid MAGs that mapped to a 16S OTU, four were visualized based on their  
316 relative abundance and spatiotemporal distributions throughout the Hainich CZE (Figure 3). The  
317 16S sequence from bin49 was full length (1498 bp) and shared 100% identity across the full  
318 OTU\_31 sequence. The MAG taxonomy (GTDB\_TK) was class ABY1 within the  
319 Patescibacteria, while the 16S taxonomy (RDP trained with SILVA v.132) was *Candidatus*  
320 *Kerfeldbacteria* within the same class (Wang *et al.*, 2007; Schloss *et al.*, 2009; Quast *et al.*,  
321 2012; Parks *et al.*, 2018). This population recently showed a large increase in relative  
322 abundance starting in Jan 2017 and is localized to well H5-2 within the upper aquifer  
323 assemblage, where these metagenomes originated from. Bin19 and bin52 also both contained  
324 partial 16S sequences (769 bp, 727 bp respectively) that were 100% identical to corresponding  
325 16S OTU sequences. The GTDB\_TK taxonomy for bin19 was within the order  
326 Peregrinibacterales (Patescibacteria) while bin52 was most similar to the MBNT15 group. One  
327 exciting finding was that both these organisms were more relatively abundant in the oxic well

328 H4-1 within the lower aquifer assemblage rather than the anoxic well that was used to generate  
329 the metagenomes. The last example provided is for a MAG, bin61, within the  
330 Thermodesulfovibrionales (Nitrospirota) that shared 99% sequence identity to the most  
331 abundant OTU detected across the entire Hainich CZE (mean  $\pm$  SD relative abundance = 5.9  $\pm$   
332 7.6%; max = 32%). This OTU is extremely abundant within the anoxic wells H53 and H52, while  
333 also being among the most abundant OTU in the oxic or hypoxic Trochitenkalk formation  
334 (moTK; HTL) at times (wells H41 and H51). With these examples, we extend the information  
335 provided by a spatially constrained metagenomics project across the entire aquifer assemblage  
336 to better explore the potential niches of these abundant organisms.

337 Unlike more traditional, gene-centric based analyzes that provide insights into the sum  
338 metabolic repertoire of an ecosystem, a genome-centric approach enables research questions  
339 directed towards population niche differentiation, determination of microbial groups that are  
340 bioindicators for a specific metabolism, and potential microbial networks and microbial  
341 interactions between syntrophs and/or auxotrophs along with the phages that control population  
342 sizes and alter or enhance biogeochemical cycling rates (Anantharaman *et al.*, 2016;  
343 Howard-Varona *et al.*, 2017). Such an approach further offers insights into the evolutionary  
344 history of archaeal, bacterial, or viral groups and the ecological consequences if such groups  
345 were to be lost or invade the system. In particular, the identification of novel viruses from  
346 metagenomic data and the way they interact with other microbes extends our understanding of  
347 complex environmental systems (Roux *et al.*, 2016). As a final consideration, the information  
348 contained within high-quality MAGs may offer a road map to cultivation, which in turn allows  
349 hypothesis testing and verification of *in silico* predictions (Cross *et al.*, 2019).

350

351

## Conclusions

352           To improve the recovery of metagenome-assembled-genomes we find that the addition  
353 of Oxford Nanopore Technology (ONT) long-read sequencing doubled the number of bacterial  
354 and archaeal MAGs, that represented more phylogenetic diversity, and improved all measured  
355 quality metrics as compared to an Illumina short-read approach only. In addition, nearly four-fold  
356 more putative phage sequences were identified including 10x more putative prophages.  
357 Considerations on supplementing Illumina paired-end metagenomic projects with ONT reads  
358 include the DNA extraction method used, the total amount of DNA available, and the cleanliness  
359 of the extract. The additional amount of hands-on time needed to prepare a sequencing run with  
360 the minION is comparably low. The current library preparation time using the revised genomic  
361 DNA by ligation kit takes about three hours (including elongated incubation times). Shorter  
362 protocols such as the rapid kit are also available by the ONT-community. A sequencing run lasts  
363 between 24 and 48 hours, or until no active pores are available anymore and the data can be  
364 immediately analyzed depending on the available hardware. There are cost concerns with  
365 supplementing an already expensive metagenomic sequencing project with ONT long-read  
366 sequences, considering a complete run on one minION flow cell, including library preparation,  
367 currently costs 750 € per sample. However, the improvements documented here provide better  
368 genome context for both microbial and viral comparative genomic projects, more single marker  
369 copy genes for detailed phylogenomic studies, more complete metabolic reconstructions, and  
370 an end-product that is more useful to the greater scientific community.



371

## Acknowledgements

372           We thank Falko Gutmann, Perla Abigail Figueroa-Gonzalez, Till Bornemann and Heiko  
373 Minkmar for water sampling and water filtration. We would also like to thank Alexander Probst  
374 for his helpful comments and discussion, and Stefan Riedel for operating the Illumina MiSeq.  
375 Martin Hölzer appreciates the support of the Joachim Herz Foundation by the add-on fellowship  
376 for interdisciplinary life science. This study was conducted within the Collaborative Research  
377 Centre AquaDiva (CRC 1076 AquaDiva) of the Friedrich Schiller University Jena, and was  
378 funded by the Deutsche Forschungsgemeinschaft.

379

380 The authors have no conflicts of interest.

381

382

## References

- 383 Al-Shayeb, B., Sachdeva, R., Chen, L.-X., Ward, F., Munk, P., Devoto, A., et al. (2019) Clades of  
384 huge phage from across Earth's ecosystems. *bioRxiv* 572362.
- 385 Altschul, S.F., Gish, W., Miller, W., Myers, E.W., and Lipman, D.J. (1990) Basic local alignment  
386 search tool. *J Mol Biol* **215**: 403–410.
- 387 Anantharaman, K., Brown, C.T., Hug, L.A., Sharon, I., Castelle, C.J., Probst, A.J., et al. (2016)  
388 Thousands of microbial genomes shed light on interconnected biogeochemical processes  
389 in an aquifer system. *Nat Commun* **7**: 13219.
- 390 Bertrand, D., Shaw, J., Kalathiyappan, M., Ng, A.H.Q., Kumar, M.S., Li, C., et al. (2019) Hybrid  
391 metagenomic assembly enables high-resolution analysis of resistance determinants and  
392 mobile elements in human microbiomes. *Nat Biotechnol* **37**: 937–944.
- 393 Bowers, R.M., Kyrpides, N.C., Stepanauskas, R., Harmon-Smith, M., Doud, D., Reddy, T.B.K.,  
394 et al. (2017) Minimum information about a single amplified genome (MISAG) and a  
395 metagenome-assembled genome (MIMAG) of bacteria and archaea. *Nat Biotechnol* **35**:  
396 725–731.
- 397 Breitbart, M., Salamon, P., Andresen, B., Mahaffy, J.M., Segall, A.M., Mead, D., et al. (2002)  
398 Genomic analysis of uncultured marine viral communities. *Proc Natl Acad Sci U S A* **99**:  
399 14250–14255.
- 400 Brown, C.T., Hug, L.A., Thomas, B.C., Sharon, I., Castelle, C.J., Singh, A., et al. (2015) Unusual  
401 biology across a group comprising more than 15% of domain Bacteria. *Nature* **523**:  
402 208–211.
- 403 Bushnell, B. (2014) BBTools software package. URL <http://sourceforge.net/projects/bbmap>.
- 404 Chen, L.-X., Anantharaman, K., Shaiber, A., Murat Eren, A., and Banfield, J.F. (2019) Accurate  
405 and Complete Genomes from Metagenomes. *bioRxiv* 808410.
- 406 Cross, K.L., Campbell, J.H., Balachandran, M., Campbell, A.G., Cooper, S.J., Griffen, A., et al.  
407 (2019) Targeted isolation and cultivation of uncultivated bacteria by reverse genomics. *Nat*  
408 *Biotechnol*.
- 409 Daims, H., Lebedeva, E.V., Pjevac, P., Han, P., Herbold, C., Albertsen, M., et al. (2015)  
410 Complete nitrification by *Nitrospira* bacteria. *Nature* **528**: 504–509.
- 411 Delmont, T.O., Quince, C., Shaiber, A., Esen, Ö.C., Lee, S.T., Rappé, M.S., et al. (2018)  
412 Nitrogen-fixing populations of Planctomycetes and Proteobacteria are abundant in surface  
413 ocean metagenomes. *Nat Microbiol* **3**: 804–813.
- 414 Devoto, A.E., Santini, J.M., Olm, M.R., Anantharaman, K., Munk, P., Tung, J., et al. (2019)  
415 Megaphages infect *Prevotella* and variants are widespread in gut microbiomes. *Nat*  
416 *Microbiol* **4**: 693–700.
- 417 Dutilh, B.E., Cassman, N., McNair, K., Sanchez, S.E., Silva, G.G.Z., Boling, L., et al. (2014) A  
418 highly abundant bacteriophage discovered in the unknown sequences of human faecal  
419 metagenomes. *Nat Commun* **5**: 4498.
- 420 Eddy, S. (2017) HMMER3: a new generation of sequence homology search software.
- 421 Frank, J.A., Pan, Y., Tooming-Klunderud, A., Eijsink, V.G.H., McHardy, A.C., Nederbragt, A.J.,  
422 and Pope, P.B. (2016) Improved metagenome assemblies and taxonomic binning using  
423 long-read circular consensus sequence data. *Sci Rep* **6**: 25373.
- 424 Fridman, S., Flores-Urbe, J., Larom, S., Alalouf, O., Liran, O., Yacoby, I., et al. (2017) A  
425 myovirus encoding both photosystem I and II proteins enhances cyclic electron flow in  
426 infected *Prochlorococcus* cells. *Nat Microbiol* **2**: 1350–1357.

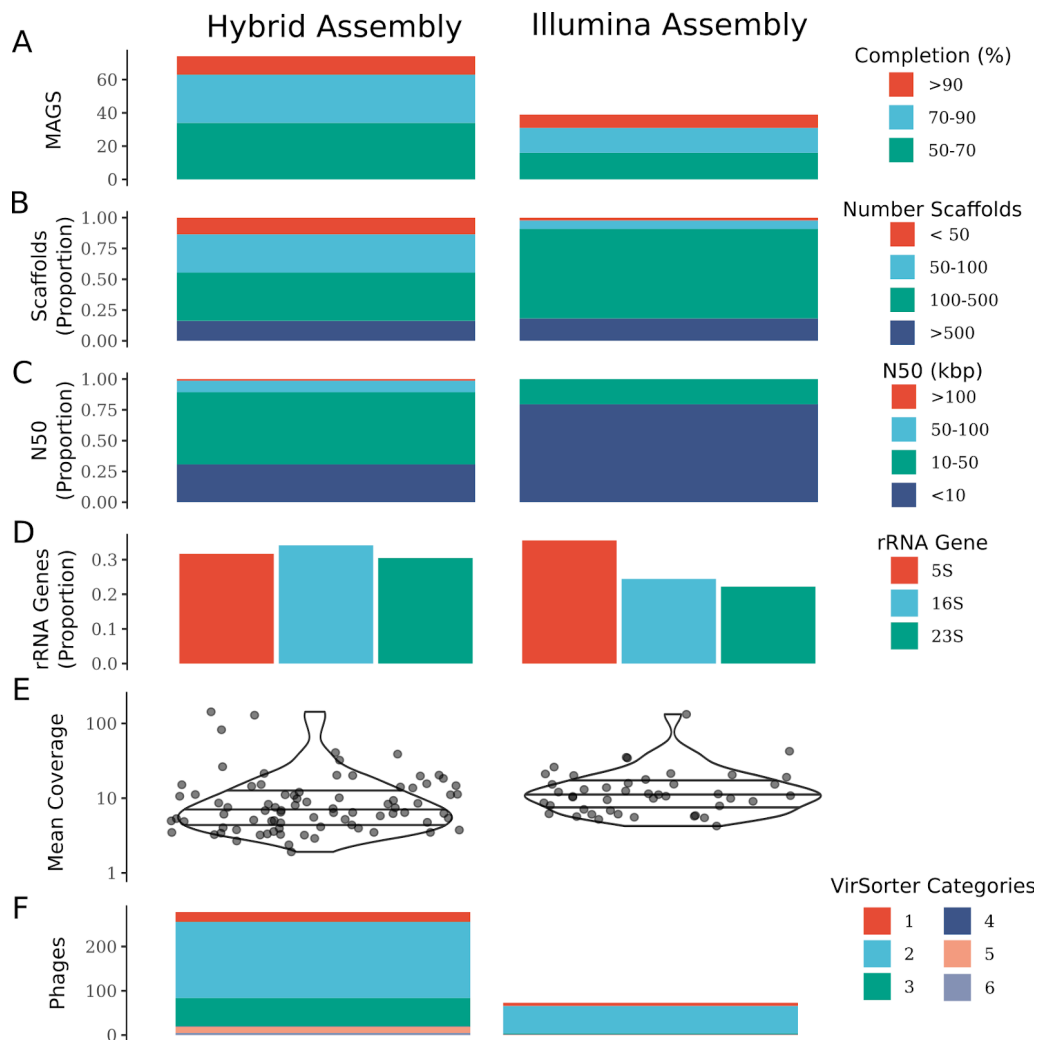
- 427 Fuhrman, J.A. (1999) Marine viruses and their biogeochemical and ecological effects. *Nature*  
428 **399**: 541–548.
- 429 Goldberg, S.M.D., Johnson, J., Busam, D., Feldblyum, T., Ferriera, S., Friedman, R., et al.  
430 (2006) A Sanger/pyrosequencing hybrid approach for the generation of high-quality draft  
431 assemblies of marine microbial genomes. *Proc Natl Acad Sci U S A* **103**: 11240–11245.
- 432 Graham, E.D., Heidelberg, J.F., and Tully, B.J. (2017) BinSanity: unsupervised clustering of  
433 environmental microbial assemblies using coverage and affinity propagation. *PeerJ* **5**:  
434 e3035.
- 435 Gutleben, J., Chaib De Mares, M., van Elsas, J.D., Smidt, H., Overmann, J., and Sipkema, D.  
436 (2018) The multi-omics promise in context: from sequence to microbial isolate. *Crit Rev*  
437 *Microbiol* **44**: 212–229.
- 438 Handelsman, J., Tiedje, J., Alvarez-Cohen, L., Ashburner, M., Cann, I.K.O., Delong, E.F., et al.  
439 (2007) *The New Science of Metagenomics : Revealing the Secrets of Our Microbial Planet*,  
440 The National Academies Press.
- 441 Herrmann, M., Wegner, C.-E., Taubert, M., Geesink, P., Lehmann, K., Yan, L., et al. (2019)  
442 Predominance of *Candidatus* Patescibacteria in Groundwater Is Caused by Their Preferential  
443 Mobilization From Soils and Flourishing Under Oligotrophic Conditions. *Front Microbiol* **10**:  
444 1407.
- 445 Howard-Varona, C., Hargreaves, K.R., Abedon, S.T., and Sullivan, M.B. (2017) Lysogeny in  
446 nature: mechanisms, impact and ecology of temperate phages. *ISME J* **11**: 1511–1520.
- 447 Hug, L.A., Baker, B.J., Anantharaman, K., Brown, C.T., Probst, A.J., Castelle, C.J., et al. (2016)  
448 A new view of the tree of life. *Nat Microbiol* **1**: 16048.
- 449 Hyatt, D., Chen, G.-L., LoCascio, P.F., Land, M.L., Larimer, F.W., and Hauser, L.J. (2010)  
450 Prodigal: prokaryotic gene recognition and translation initiation site identification. *BMC*  
451 *Bioinformatics* **11**: 119.
- 452 Imachi, H., Nobu, M.K., Nakahara, N., Morono, Y., Ogawara, M., Takaki, Y., et al. (2019)  
453 Isolation of an archaeon at the prokaryote-eukaryote interface. *bioRxiv*.
- 454 Jain, C., Rodriguez-R, L.M., Phillippy, A.M., Konstantinidis, K.T., and Aluru, S. (2018) High  
455 throughput ANI analysis of 90K prokaryotic genomes reveals clear species boundaries. *Nat*  
456 *Commun* **9**: 5114.
- 457 Kallies, R., Hölzer, M., Brizola Toscan, R., Nunes da Rocha, U., Anders, J., Marz, M., and  
458 Chatzinotas, A. (2019) Evaluation of Sequencing Library Preparation Protocols for Viral  
459 Metagenomic Analysis from Pristine Aquifer Groundwaters. *Viruses* **11**:
- 460 Kang, D.D., Froula, J., Egan, R., and Wang, Z. (2015) MetaBAT, an efficient tool for accurately  
461 reconstructing single genomes from complex microbial communities. *PeerJ* **3**: e1165.
- 462 Kang, D., Li, F., Kirton, E.S., Thomas, A., Egan, R.S., An, H., and Wang, Z. (2019) MetaBAT 2:  
463 an adaptive binning algorithm for robust and efficient genome reconstruction from  
464 metagenome assemblies, *PeerJ Preprints*.
- 465 Kohlhepp, B., Lehmann, R., Seeber, P., Küsel, K., Trumbore, S.E., and Totsche, K.U. (2017)  
466 Aquifer configuration and geostructural links control the groundwater quality in thin-bedded  
467 carbonate–siliciclastic alternations of the Hainich CZE, central Germany. *Hydrol Earth Syst*  
468 *Sci* **21**: 6091–6116.
- 469 Kurtz, S., Phillippy, A., Delcher, A.L., Smoot, M., Shumway, M., Antonescu, C., and Salzberg,  
470 S.L. (2004) Versatile and open software for comparing large genomes. *Genome Biol* **5**:  
471 R12.
- 472 Küsel, K., Totsche, K.U., Trumbore, S.E., Lehmann, R., Steinhäuser, C., and Herrmann, M.  
473 (2016) How Deep Can Surface Signals Be Traced in the Critical Zone? Merging Biodiversity  
474 with Biogeochemistry Research in a Central German Muschelkalk Landscape. *Front Earth*

- Sci Chin* **4**: 32.
- Lehmann, R. and Totsche, K.U. (2020) Multi-directional flow dynamics shape groundwater quality in sloping bedrock strata. *J Hydrol* **580**: 124291.
- Li, H. (2018) Minimap2: pairwise alignment for nucleotide sequences. *Bioinformatics* **34**: 3094–3100.
- Li, H., Handsaker, B., Wysoker, A., Fennell, T., Ruan, J., Homer, N., et al. (2009) The sequence alignment/map format and SAMtools. *Bioinformatics* **25**: 2078–2079.
- Luo, C., Tsementzi, D., Kyripides, N.C., and Konstantinidis, K.T. (2012) Individual genome assembly from complex community short-read metagenomic datasets. *ISME J* **6**: 898–901.
- Matsen, F.A., Kodner, R.B., and Armbrust, E.V. (2010) pplacer: linear time maximum-likelihood and Bayesian phylogenetic placement of sequences onto a fixed reference tree. *BMC Bioinformatics* **11**: 538.
- Mikheenko, A., Saveliev, V., and Gurevich, A. (2016) MetaQUAST: evaluation of metagenome assemblies. *Bioinformatics* **32**: 1088–1090.
- Murat Eren, A., Esen, Ö.C., Quince, C., Vineis, J.H., Morrison, H.G., Sogin, M.L., and Delmont, T.O. (2015) Anvi'o: an advanced analysis and visualization platform for 'omics data. *PeerJ* **3**: e1319.
- Nooij, S., Schmitz, D., Vennema, H., Kroneman, A., and Koopmans, M.P.G. (2018) Overview of Virus Metagenomic Classification Methods and Their Biological Applications. *Front Microbiol* **9**: 749.
- Nurk, S., Meleshko, D., Korobeynikov, A., and Pevzner, P.A. (2017) metaSPAdes: a new versatile metagenomic assembler. *Genome Res* **27**: 824–834.
- Parks, D.H., Chuvochina, M., Waite, D.W., Rinke, C., Skarshewski, A., Chaumeil, P.-A., and Hugenholtz, P. (2018) A standardized bacterial taxonomy based on genome phylogeny substantially revises the tree of life. *Nat Biotechnol* **36**: 996–1004.
- Parks, D.H., Imelfort, M., Skennerton, C.T., Hugenholtz, P., and Tyson, G.W. (2015) CheckM: assessing the quality of microbial genomes recovered from isolates, single cells, and metagenomes. *Genome Res* **25**: 1043–1055.
- Paulson, J.N., Stine, O.C., Bravo, H.C., and Pop, M. (2013) Differential abundance analysis for microbial marker-gene surveys. *Nat Methods* **10**: 1200–1202.
- Pedron, R., Esposito, A., Bianconi, I., Pasolli, E., Tett, A., Asnicar, F., et al. (2019) Genomic and metagenomic insights into the microbial community of a thermal spring. *Microbiome* **7**: 8.
- Price, M.N., Dehal, P.S., and Arkin, A.P. (2010) FastTree 2 – Approximately Maximum-Likelihood Trees for Large Alignments. *PLoS One* **5**: e9490.
- Quast, C., Pruesse, E., Yilmaz, P., Gerken, J., Schweer, T., Yarza, P., et al. (2012) The SILVA ribosomal RNA gene database project: improved data processing and web-based tools. *Nucleic Acids Res* **41**: D590–D596.
- R Core Team (2014) R: A Language and Environment for Statistical Computing.
- Roux, S., Brum, J.R., Dutilh, B.E., Sunagawa, S., Duhaime, M.B., Loy, A., et al. (2016) Ecogenomics and potential biogeochemical impacts of globally abundant ocean viruses. *Nature* **537**: 689–693.
- Roux, S., Enault, F., Hurwitz, B.L., and Sullivan, M.B. (2015) VirSorter: mining viral signal from microbial genomic data. *PeerJ* **3**: e985.
- Schloss, P.D., Westcott, S.L., Ryabin, T., Hall, J.R., Hartmann, M., Hollister, E.B., et al. (2009) Introducing mothur: Open-source, platform-independent, community-supported software for describing and comparing microbial communities. *Appl Environ Microbiol* **75**: 7537–7541.
- Scholz, M., Lo, C.-C., and Chain, P.S.G. (2014) Improved assemblies using a source-agnostic pipeline for MetaGenomic Assembly by Merging (MeGAMerge) of contigs. *Sci Rep* **4**: 6480.

- 523 Seemann, T. (2015) Barnap.  
524 Shaiber, A. and Eren, A.M. (2019) Composite Metagenome-Assembled Genomes Reduce the  
525 Quality of Public Genome Repositories. *MBio* **10**.  
526 Taubert, M., Stöckel, S., Geesink, P., Girus, S., Jehmlich, N., von Bergen, M., et al. (2018)  
527 Tracking active groundwater microbes with D2O labelling to understand their ecosystem  
528 function. *Environ Microbiol* **20**: 369–384.  
529 Tyson, G.W., Chapman, J., Hugenholtz, P., Allen, E.E., Ram, R.J., Richardson, P.M., et al.  
530 (2004) Community structure and metabolism through reconstruction of microbial genomes  
531 from the environment. *Nature* **428**: 37–43.  
532 Uritskiy, G.V., DiRuggiero, J., and Taylor, J. (2018) MetaWRAP-a flexible pipeline for  
533 genome-resolved metagenomic data analysis. *Microbiome* **6**: 158.  
534 Venter, J.C., Remington, K., Heidelberg, J.F., Halpern, A.L., Rusch, D., Eisen, J.A., et al. (2004)  
535 Environmental genome shotgun sequencing of the Sargasso Sea. *Science* **304**: 66–74.  
536 Wang, Q., Garrity, G.M., Tiedje, J.M., and Cole, J.R. (2007) Naïve Bayesian Classifier for Rapid  
537 Assignment of rRNA Sequences into the New Bacterial Taxonomy. *Appl Environ Microbiol*  
538 **73**: 5261–5267.  
539 Wegner, C.-E., Gaspar, M., Geesink, P., Herrmann, M., Marz, M., and Küsel, K. (2019)  
540 Biogeochemical Regimes in Shallow Aquifers Reflect the Metabolic Coupling of the  
541 Elements Nitrogen, Sulfur, and Carbon. *Appl Environ Microbiol* **85**.  
542 Wickham, H. (2009) ggplot2: elegant graphics for data analysis, Springer New York.  
543 Wickham, H., Averick, M., Bryan, J., Chang, W., McGowan, L., François, R., et al. (2019)  
544 Welcome to the Tidyverse. *Journal of Open Source Software* **4**: 1686.  
545 Woyke, T., Doud, D.F.R., and Elie-Fadrosh, E.A. (2019) Genomes From Uncultivated  
546 Microorganisms. *Encyclopedia of Microbiology*, 4e.  
547 Wu, Y.-W., Simmons, B.A., and Singer, S.W. (2016) MaxBin 2.0: an automated binning algorithm  
548 to recover genomes from multiple metagenomic datasets. *Bioinformatics* **32**: 605–607.  
549 Yan, L., Herrmann, M., Kampe, B., Lehmann, R., Totsche, K.U., and Küsel, K. (2019)  
550 Environmental selection shapes the formation of near-surface groundwater microbiomes.  
551 *Water Res* **170**: 115341.

552

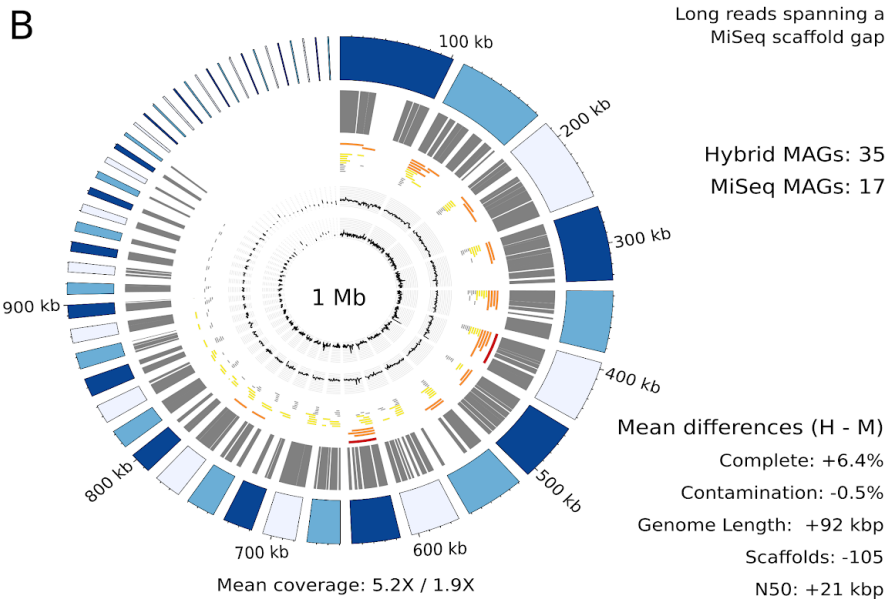
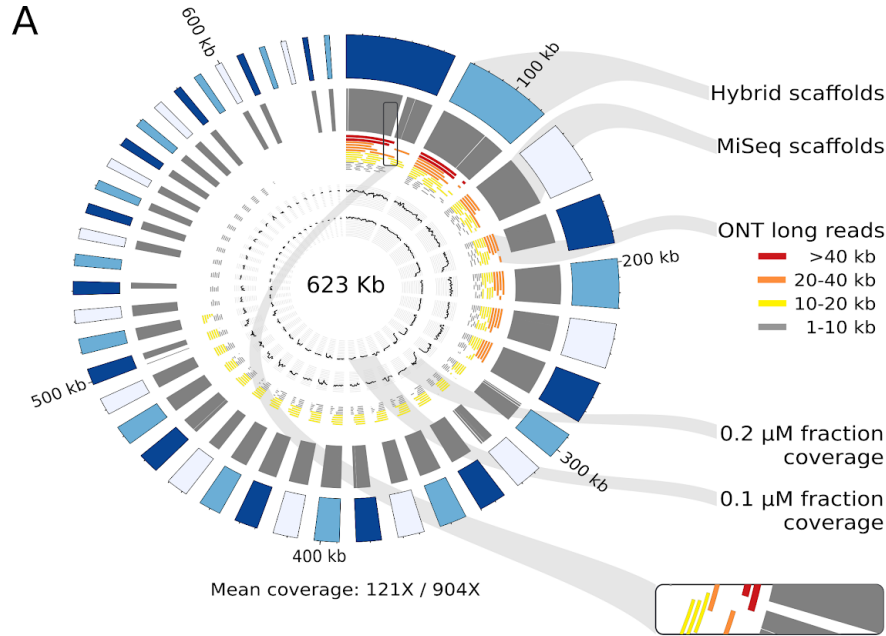
553



554 Figure 1. Genome metrics for all MAGs that were > 50% complete and < 10% redundant  
 555 reconstructed from the hybrid assembly (left) and the Illumina-only assembly (right). (A) The  
 556 number of MAGs from each method. (B) The number of scaffolds each MAG was represented  
 557 by relative to all recovered MAGs. (C) The N50 value for each MAG recovered as a proportion  
 558 of all MAGs. (D) The proportion of MAGs containing each of the rRNA genes. (E) The mean  
 559 coverage of every MAG that met our quality standards within each approach (points) and their  
 560 distributions plotted on a log10 scale. (F) The number of identified phages / prophages in each  
 561 assembly as assessed with VirSorter.  
 562



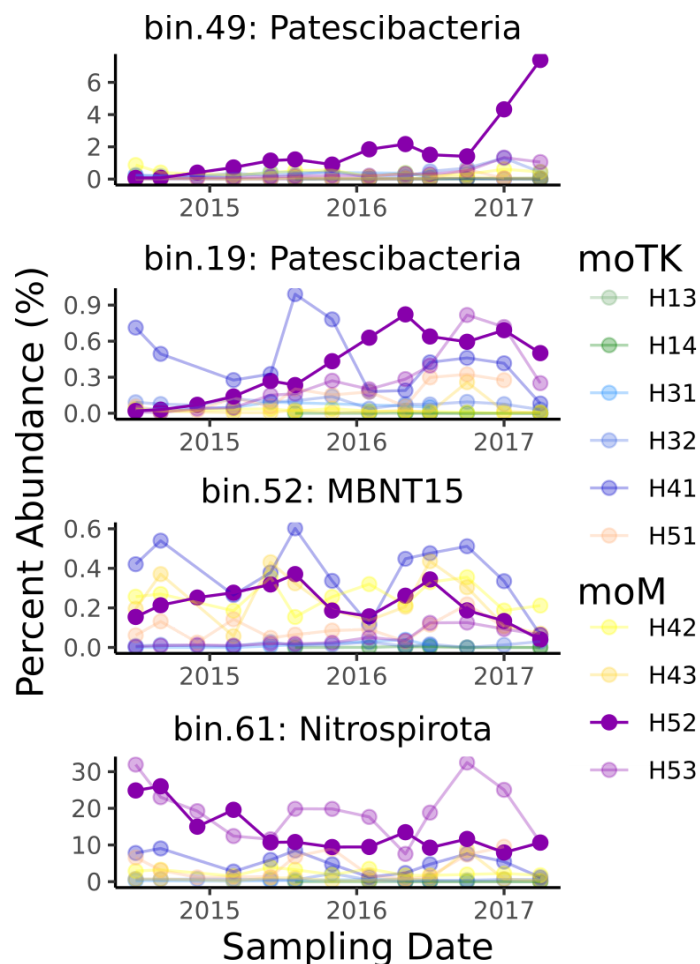
563



564 Figure 2. Genome circos plots for the most (A) and least (B) covered Patescibacteria MAGs  
 565 retrieved by both assembly methods. The outer ring in blue represents the hybrid assembly  
 566 derived scaffolds, followed by the corresponding Illumina assembly scaffolds in grey. The  
 567 nanopore reads were mapped with minimap2 and colored based on length. The coverage  
 568 values are log<sub>2</sub> scaled and calculated for each 1kb segment of the hybrid-derived scaffolds with  
 569 pileup.sh from BBTools of the Illumina reads. The values below each plot represent the mean  
 570 coverage from the 0.2  $\mu$ M fraction Illumina MiSeq reads and the 0.1  $\mu$ M fraction reads,  
 571 respectively. The hybrid based genome size is indicated in the middle of each plot.

572  
573

574



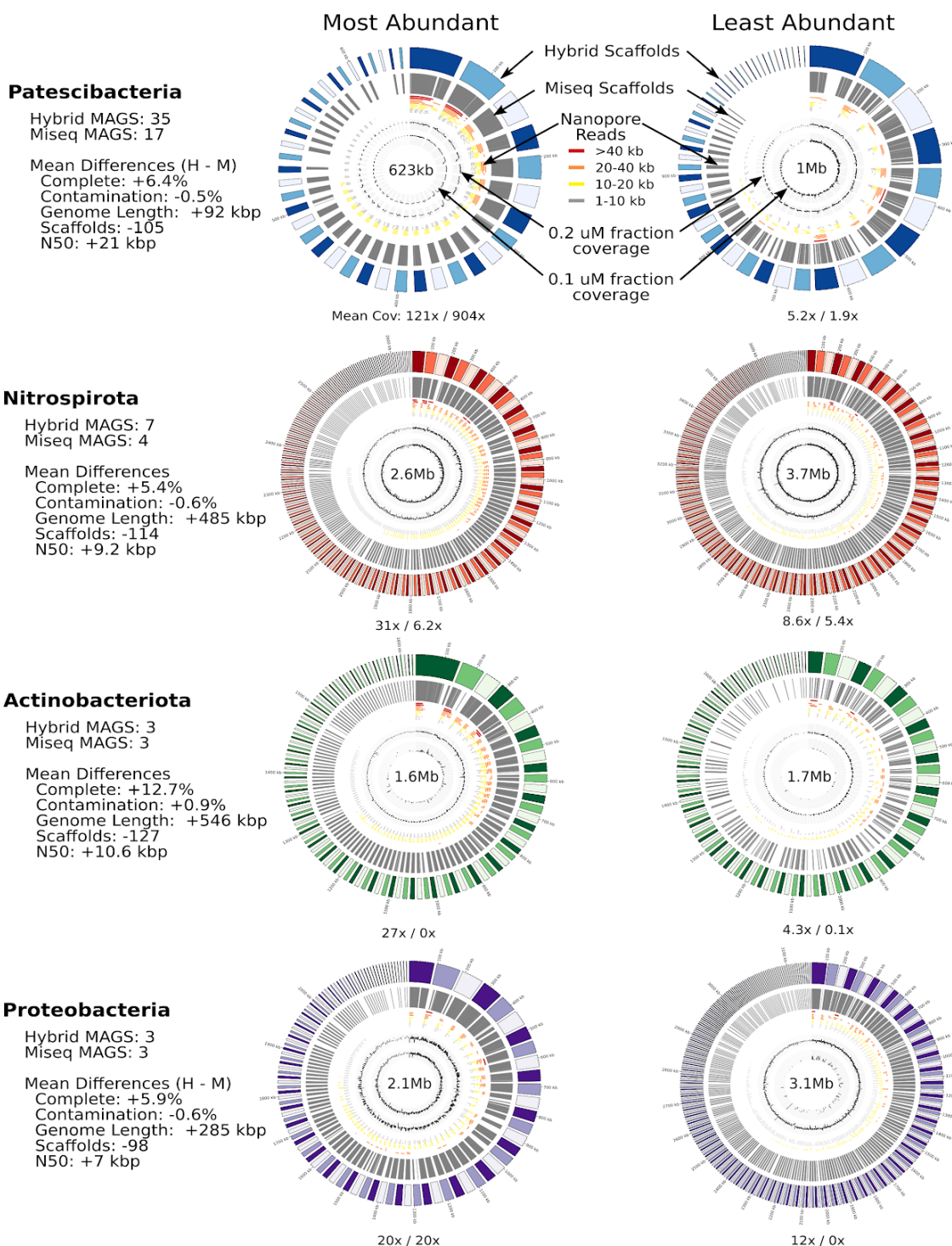
575 Figure 3. MAGs containing 16S genes were mapped to the amplicon sequence dataset  
 576 presented in Yan et al., using blastn. All matches were > 99% sequence identity across at least  
 577 350 bp. The distribution of these OTU was explored throughout the full aquifer system across a  
 578 3-year monthly sampling time series. The aquifer is mainly divided into two assemblages, the  
 579 upper (moM; HTU) characterized by anoxia, and the lower (moTK; HTL) by oxic and hypoxic  
 580 conditions. H52 was the well where the DNA for the metagenomes originated from and is  
 581 highlighted with the solid purple. The percent abundance values result from counts that were  
 582 normalized with metagenomeseq (Paulson *et al.*, 2013). The mapping information is as follows:  
 583 bin.49 (len = 1498 bp; ID = 100%, 404 bp); bin.19 (len = 769, ID = 100%, 405 bp); bin.52 (len =  
 584 769, ID = 100%, 405 bp); bin.61 (len = 1403; 99%, 402 bp). All 16S and MAG taxonomic  
 585 assignments were consistent.

586

587



588



589 Figure S1. Genome circos plots for the most (left) and least (right) covered MAGs from four  
 590 phyla previously demonstrated to be abundant and important in biogeochemical cycling in the  
 591 Hainich CZE. The outer ring of each plot represents the hybrid assembly derived scaffolds,  
 592 followed by the corresponding Illumina assembly scaffolds in grey. The ONT long reads were  
 mapped with minimap2 and colored based on length. The coverage values are log2 scaled and

593 calculated for each 1kb segment of the hybrid-derived scaffolds with pileup.sh from BBTools.  
594 The values below each plot represent the mean coverage from the 0.2  $\mu$ M fraction Illumina  
595 MiSeq reads and the 0.1  $\mu$ M fraction reads, respectively. The hybrid based genome size is  
596 indicated in the middle of each plot.

597  
598  
599 Table S1. Comparison of the MAGs (bins) that were recovered in both the hybrid and  
600 Illumina-only (Miseq) based analyses.  
601 [https://docs.google.com/spreadsheets/d/1AsoGrB6wfRGWqE6ToRQoHR8AWJq97A16\\_5UP-71](https://docs.google.com/spreadsheets/d/1AsoGrB6wfRGWqE6ToRQoHR8AWJq97A16_5UP-717c_0/edit#gid=2054870087)  
602 [7c\\_0/edit#gid=2054870087](https://docs.google.com/spreadsheets/d/1AsoGrB6wfRGWqE6ToRQoHR8AWJq97A16_5UP-717c_0/edit#gid=2054870087)

603  
604 Table S2. The effect of subsampling the ONT reads on the number of MAGs that were > 50%  
605 complete and < 10% redundant (as assessed by checkM).

	ONT Seqs (n)	ONT Gbp	Number MAGs*	Number Shared MAGs**
Full Hybrid	2380279	12.6	82	74 <sup>a</sup>
Nanopore > 10000	349321	6.8	76	69
Nanopore > 20000	114853	3.6	70	61
Nanopore > 50000	7848	0.48	58	53
25% Nanopore	595070	3.15	62	57
Illumina Only	0	0	44	39

606 \*This was the total number of MAGs recovered from the refinement of the automated binners.

607 \*\*The number of MAGs recovered with each method that were also recovered from the  
608 full-hybrid method.

609 <sup>a</sup>The drop from 82 to 74 MAGs within full-hybrid method was due to differences in the  
610 redundancy/completeness estimates between Anvi'o and checkM and we opted to only include  
611 those that passed both metrics.